

Research Article

Comparative Pharmacokinetic Study of Taxifolin after Oral Administration of Fructus Polygoni Orientalis Extract in Normal and Fibrotic Rats by UPLC-MS/MS

Feili Wei,^{1,2,3} Li Guo,^{1,2} Yongsong Xu,^{1,2} Dexi Chen ³ and Muxin Gong ^{1,2}

¹School of Traditional Chinese Medicine, Capital Medical University, Beijing 100069, China

²Beijing Key Lab of TCM Collateral Disease Theory Research, Beijing 100069, China

³Beijing Institute of Hepatology, Beijing Youan Hospital, Capital Medical University, Beijing 100069, China

Correspondence should be addressed to Muxin Gong; gongmuxin@126.com

Received 26 July 2019; Revised 28 November 2019; Accepted 4 December 2019; Published 31 December 2019

Academic Editor: Michał Tomczyk

Copyright © 2019 Feili Wei et al. This is an open access article distributed under the Creative Commons Attribution License, which permits unrestricted use, distribution, and reproduction in any medium, provided the original work is properly cited.

Fructus polygoni orientalis (FPO) is widely used in clinical practice in China, especially in treatment of liver diseases including viral hepatitis, liver fibrosis, and liver cirrhosis. However, its pharmacokinetic (PK) alterations in liver fibrotic rats have rarely been reported. To study whether taxifolin, one of the main flavonoids in FPO can be absorbed into blood after oral administration of FPO extract and to compare the differences in pharmacokinetic parameters of taxifolin to normal and liver fibrotic rats induced by porcine serum (PS), a UPLC-MS/MS method was developed and validated for determination of taxifolin in rat plasma using puerarin as the internal standard (IS). All validation parameters met the acceptance criteria according to regulatory guidelines. The results indicated that after treatment of rats with PS alone for 12 weeks, the liver fibrotic model group was built successfully. The taxifolin can be absorbed into the blood after oral administration of the FPO extract. The C_{max} of taxifolin was 1940 ± 502.2 ng/mL and 2648 ± 208.5 ng/mL ($p < 0.05$), the AUC_{0-t} of taxifolin was 4949.7 ± 764.89 h-ng/mL and 6679.9 ± 734.26 h-ng/mL ($p < 0.05$), the $AUC_{0-\infty}$ of taxifolin was 5049.4 ± 760.7 and 7095.2 ± 962.3 h-ng/mL ($p < 0.05$), and the mean residence time (MRT) of taxifolin was 2.46 ± 0.412 h and 3.17 ± 0.039 h ($p < 0.05$) in the normal and fibrotic model groups, respectively. These results confirmed that the pharmacokinetic parameters of taxifolin are altered in liver fibrosis, manifested as C_{max} , AUC_{0-t} , $AUC_{0-\infty}$, and the mean residence time (MRT). It suggested that it is essential to consider the characteristics of pharmacokinetics after oral administration of FPO in liver disease patients.

1. Introduction

Liver fibrosis is a common pathological stage in chronic liver injury caused by various factors that leads to the accumulation of extracellular matrix (ECM) and formation of fibrous scars [1–3].

Disruption of the liver structure by fibrous scars can result in the loss of hepatocyte cells and deregulation of normal liver functions and can ultimately develop into cirrhosis and liver failure [4, 5]. Animal experiments and clinical studies have shown that liver fibrosis, even early cirrhosis, is reversible [6, 7]. Combined treatment of etiology and fibrosis can accelerate the decline of liver fibrosis and promote liver regeneration [6, 8]. At present, many potential

antifibrosis targets have been discovered through animal experiments, but most are still in the clinical trial stage [9–11].

As a traditional Chinese medicinal herb, FPO is the dried and mature fruit of *Polygonum orientale* L. It has been used in China for the treatment of various liver diseases such as hepatitis, liver fibrosis, and cirrhosis [12]. Taxifolin, also known as dihydroquercetin, is one of the most abundant flavonoids in FPO and has been listed as an indicator of quality for FPO in the Chinese Pharmacopeia 2015 edition [13, 14]. Studies have found that taxifolin possesses hepatoprotective properties, which are attributed to its ability to reduce oxidative stress and to inhibit the release of inflammatory mediators [15–17]. However, whether taxifolin

can be absorbed into the blood after oral administration of FPO extract remains unclear.

The liver is a complex organ with the ability to influence drug pharmacokinetics [18]. Liver diseases can impact the PK of all drugs including absorption, distribution, metabolism, and elimination, especially when liver fibrosis is serious [19, 20]. A previous study showed that compared with healthy controls, the risk of exposure to pantoprazole in cirrhotic patients increased 5–8 times owing to decreased liver clearance [21].

The objective of this study was to establish and validate a sensitive and selective UPLC-MS/MS method and then to apply the method to pharmacokinetic comparison between normal and liver fibrotic rats after oral administration of FPO extract. We hope the results can provide meaningful reference information for FPO usage and for development of a safe and effective medication.

2. Experimental

2.1. Chemicals and Reagents. The FPO, batch no. 14053001, was purchased from the Beijing Tongrentang Pharmacy. After being crushed, FPO was refluxed three times by 70% (v/v) ethanol (2 h each at 70°C). After filtration, the alcohol extract was concentrated under reduced pressure at 45°C and then vacuumed to dryness at 80°C. Finally, the FPO extract was obtained as a brown powder. The porcine serum was obtained from Gibco (Gibco, New Zealand). The rat liver function and serum liver fibrosis indexes test kits were obtained from Nanjing Jiancheng Bioengineering Institute (Nanjing, China). The qRT-PCR reagent was obtained from TAKARA Bio Inc (DaLian, China), and the primer sequence was as described previously [22]. The reference standard of taxifolin (purity $\geq 98\%$, batch no. 111816-201102, chemical structure shown in Figure 1(a), stored at 4°C) and reference standard of puerarin (IS, purity $\geq 98\%$, batch no. 110752-201615, chemical structure shown in Figure 1(b), stored at 4°C) were both obtained from National Institutes for Food and Drug Control (Beijing, China). HPLC-grade acetonitrile and methanol were purchased from Fisher Scientific (Fair Lawn, NJ, USA). The other chemicals and reagents were of the highest grade commercially available.

2.2. Animals. Forty-two male Wistar rats (200 ± 20 g) were obtained from Beijing Vital River Laboratories Co., Ltd (Beijing, China). Following acclimatization for 1 week after arrival, thirty-six rats were used for evaluation of the efficacy and mechanism of FPO extract (data will show in another articles). Six rats were used in this comparative pharmacokinetic study. The six rats were randomly divided into normal and fibrotic groups ($n = 3$). The fibrotic group received 0.5 mL porcine serum twice a week for 12 weeks via intraperitoneal injection. At the same time, rats in the normal group were administered with the same volume of saline. The animals were housed in a temperature- and humidity-controlled environment with a 12:12 light-dark cycle and given free access to food and water. The ethics review was approved by the ethics committee of Capital

Medical University with the ethics number AEEI-2014-128 (Beijing, China). In order to examine whether treatment of rats with PS alone for 12 weeks could induce hepatic fibrosis, liver function, and serum liver fibrosis indexes were detected by ELISA, the mRNA expression level of α SMA, Collagen1A1, and Collagen3A1 in liver tissues was measured by qRT-PCR, and liver condition was assessed by haematoxylin and eosin (H&E) and Masson's trichrome staining.

2.3. Chromatographic Conditions. A UPLC system equipped with an Agilent 1290 Bin Pump and a 1290 autosampler along with a 1290 TCC column oven (Agilent Technologies, Santa Clara, USA) were used in the study. Chromatographic separation was performed on an Agilent SB-C18 column ($50 \text{ mm} \times 2.1 \text{ mm}$, $1.8 \mu\text{m}$) with a gradient elution by a mobile phase consisting of water containing 0.3% acetic acid (A) and acetonitrile containing 0.1% formic acid (B), which were filtered through a $0.45 \mu\text{m}$ membrane filter and then degassed ultrasonically for 10 min. The gradient was as follows: 0.00 min 10% B, 0.50 min 10% B, 1.00 min 70% B, 3.00 min 98% B, 3.01 min 10% B, and 5.00 min 10% B, with a flow rate of 0.30 mL/min. The injection volume was set to 1 μL . An API 6500 Qtrap mass spectrometer (Applied Biosystems/MDS Sciex, Concord, ON, Canada) was coupled with the UPLC system via a Turbo Ionspray ionization interface. The ESI source was operated in negative mode, and the curtain gases GS1 and GS2 were set at 20, 55, and 55 psi, respectively, following optimization of the setting parameters. The source temperature was set to 550°C, and the ionspray needle voltage was -4500 V . The mass spectrometer was operated at unit resolution for Q1 and low resolution for Q3 in the multiple reaction monitoring (MRM) mode, with a dwell time of 150 ms per multiple reaction monitoring channel (msec). The main MS parameters for taxifolin and puerarin (IS) are shown in Table 1. Analyst Data Acquisition and Processing software (Version 1.6.2, Applied Biosystems/MDS Sciex, Concord, ON, Canada) was used to collect and analyze the data.

2.4. Calibration Standards and Quality Control Samples. Stock solutions of taxifolin were prepared in ultrapure methanol at 2 mg/mL, and then a series of standard working solutions was prepared by diluting the appropriate amount of stock solution with ultrapure methanol to concentrations of 10–5000 ng/mL. A total of 1 mg/mL of IS solution was prepared in methanol:acetonitrile (50:50, v/v). The calibration standards were prepared by spiking 5 μL of the corresponding taxifolin working solutions into 50 μL of blank rat plasma to yield concentrations of 10, 50, 100, 500, 1000, 2000, 4000, and 5000 ng/mL. Quality control (QC) samples at low, medium, and high levels were prepared in the same way as the calibration samples to reach concentrations of 50, 1000, and 4000 ng/mL. All the calibration and QC samples were freshly prepared before analysis and stored at 4°C.

2.5. Sample Preparation. The QC samples, calibration standards samples, blank plasma samples (plasma samples got from the same batch of rat without any administration),

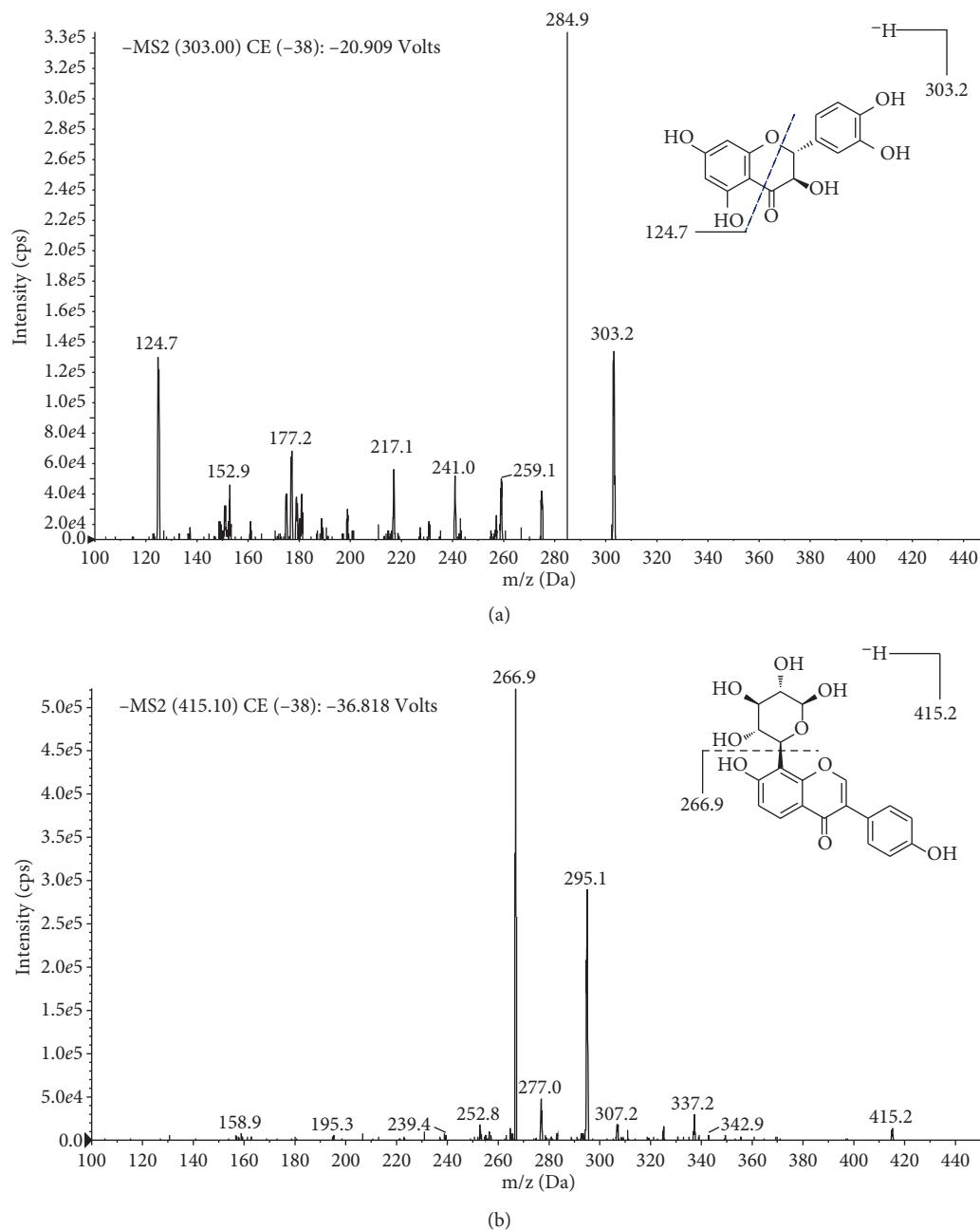


FIGURE 1: Full-scan product ion spectra of $[M + H]^+$ ions and fragmentation schemes for (a) taxifolin and (b) puerarin (internal standard).

and experimental rat samples were extracted using a protein precipitation procedure. First, these samples were thawed at room temperature for about 30 min and vortexed for 30 s. Aliquots of 50 μL rat plasma were mixed with 5 μL of methanol (or standards or QC solutions) and 200 μL of IS solution (200 ng/mL puerarin in methanol:acetonitrile (50:50, v/v)). After being vortexed for 1 min and then centrifuged at 12,000 $\times g$ for 10 min, aliquots of 130 μL supernatants were transferred to UPLC vials. An aliquot of 1 μL of sample was then injected into the UPLC-MS/MS.

2.6. Method Validation. The method was validated in compliance with the International Guidelines from the U.S.

Department of Health and Human Services Food and Drug Administration (US FDA) [23–25].

2.6.1. Selectivity. The specificity and selectivity of the UPLC-MS/MS method were evaluated by comparing six blank plasma samples from different sources with the corresponding spiked QC. The normal and fibrotic rat plasma samples were extracted after oral administration.

2.6.2. Linearity. Calibration curves were acquired through analysis of eight standards in plasma samples and plotting of the peak-area ratio of the taxifolin and IS (puerarin) versus

TABLE 1: MS parameters^a of taxifolin and puerarin (IS) determined by UPLC-MS/MS.

MS parameters	Taxifolin	Puerarin (IS)
Parent ion (<i>m/z</i>)	303.2	415.2
Product (<i>m/z</i>)	124.7	266.9
DP (V)	-120	-130
CE (eV)	-20.909	-36.818
CXP (V)		-13
Ionspray (V)		-4500
CUR (psi)		20
GS1 (psi)		55
GS2 (psi)		55
CAD (psi)		Medium
Source temperature		550

^aDP: declustering potential; CE: collision energy; CXP: cell exit potential; CAD: collision-activated dissociation.

the corresponding taxifolin concentrations (10, 50, 100, 500, 1000, 2000, 4000, and 5000 ng/mL).

2.6.3. Precision and Accuracy. To determine the intraday precision of the method, three plasma samples with concentrations of 10, 1000, and 4000 ng/mL were analyzed six times on the same day. To determine the interday precision and the accuracy, other three plasma samples with concentrations of 10, 1000, and 4000 ng/mL were run on each of three different days.

2.6.4. Extraction Recovery and Matrix Effect. The matrix effects were expressed as the mean of the peak-area ratios of the blank plasma samples spiked with taxifolin after protein precipitation divided by the injected working solution with taxifolin at the same QC concentration.

2.6.5. Stability. The stability of taxifolin in rat plasma was evaluated using three concentrations of QCs in triplicate. The stability of the prepared plasma samples was assessed after (A) incubating the samples at room temperature for 24 h followed by (B) three freeze-thaw cycles and (C) storage at -80°C for a month.

2.7. Application to Pharmacokinetics Comparison. The FPO extract was prepared by dissolution in distilled water. All rats were fasted for 12 h with free access to water before the experiments. The fibrotic rats were orally administrated with the FPO extract at a dose of 1.23 g/kg (equivalent to 52.5 mg/kg for taxifolin). The normal rats were administrated with the same volume of saline. Approximately, 300 μL of blood samples were collected from the suborbital vein into a heparinized 1.5 mL centrifuge tube at 0.083, 0.167, 0.33, 0.50, 1.0, 2.0, 4.0, 8.0, 12, and 24 h after oral administration.

2.8. Statistical Analyses. All results were expressed as the arithmetic mean plus standard deviation (SD) and analyzed using SPSS 17.0 statistical software (SPSS Inc., Chicago, IL, USA). The analysis of variance (ANOVA) was used for

comparison between groups. DAS Version 2.0 (Chinese Pharmacological Society, Beijing, China) was employed to analyze pharmacokinetic parameters including half-life ($t_{1/2}$), maximum plasma time (T_{max}) and concentration (C_{max}), area under the concentration-time curve (AUC_{0-t} and $\text{AUC}_{0-\infty}$), clearance (CL), steady-state volume of distribution (V_z), and mean residence time (MRT) by noncompartmental methods. A value of $p < 0.05$ was considered statistically significant.

3. Results

3.1. Optimization of UPLC-MS/MS Conditions. This study first described the development of a sensitive and specific UPLC-MS/MS assay for the determination of taxifolin concentrations in rat plasma after oral administration of FPO extract. The full-scan product ion mass spectra of taxifolin and puerarin (internal standard; IS) are shown in Figure 1. Mass chromatograms of taxifolin and IS obtained by extraction of blank rat plasma, blank plasma spiked with taxifolin and IS, and actual unknown plasma samples obtained in rats after oral administration of FPO extract are shown in Figure 2. The chromatographic run time for the extracted plasma samples was 5.0 min. The retention times for taxifolin and IS were 1.60 and 1.51 min, respectively. The chromatograms showed baseline separation of taxifolin and the IS without any interference from endogenous plasma components.

3.2. Characteristics of Liver Fibrosis in Model Group

3.2.1. Liver Function and Serum Liver Fibrosis Indexes after PS Treatment for 12 Weeks. Compared with the normal group, the liver function including ALT and AST showed a significantly elevated value ($p < 0.05$). The serum liver fibrosis indexes level of hyaluronic acid (HA), laminin (LN), type IV collagen (IV-C), and type III procollagen (PCIII) in the model group were significantly higher than in the normal group, and the results were shown in Table 2.

3.2.2. The mRNA Expression Level of *aSMA*, *Collagen1A1*, and *Collagen3A1* in Liver Tissues after PS Treatment for 12 Weeks. As demonstrated in Figure 3, the fold change of mRNA expression level of 3 fibrosis-related genes include *aSMA*, *Collagen1A1*, and *Collagen3A1* in liver tissues was significantly upregulated when compared with the normal live tissues ($p < 0.05$).

3.2.3. Histopathological Manifestation in PS-Induced Liver Fibrosis. The haematoxylin and eosin (H&E) and Masson's trichrome staining results showed that in normal rat groups, no obvious hepatocellular injury was found, in contrast, inflammatory cells infiltration, necrosis were clear in the model group. The Masson's trichrome staining showed that thick fibrotic septa connecting portal tracts, delimiting the classic liver lobule, and the hepatic lobules were encysted and separated by collagen bundles. The degree of rat liver fibrosis determined by microscopy at 12 weeks was at

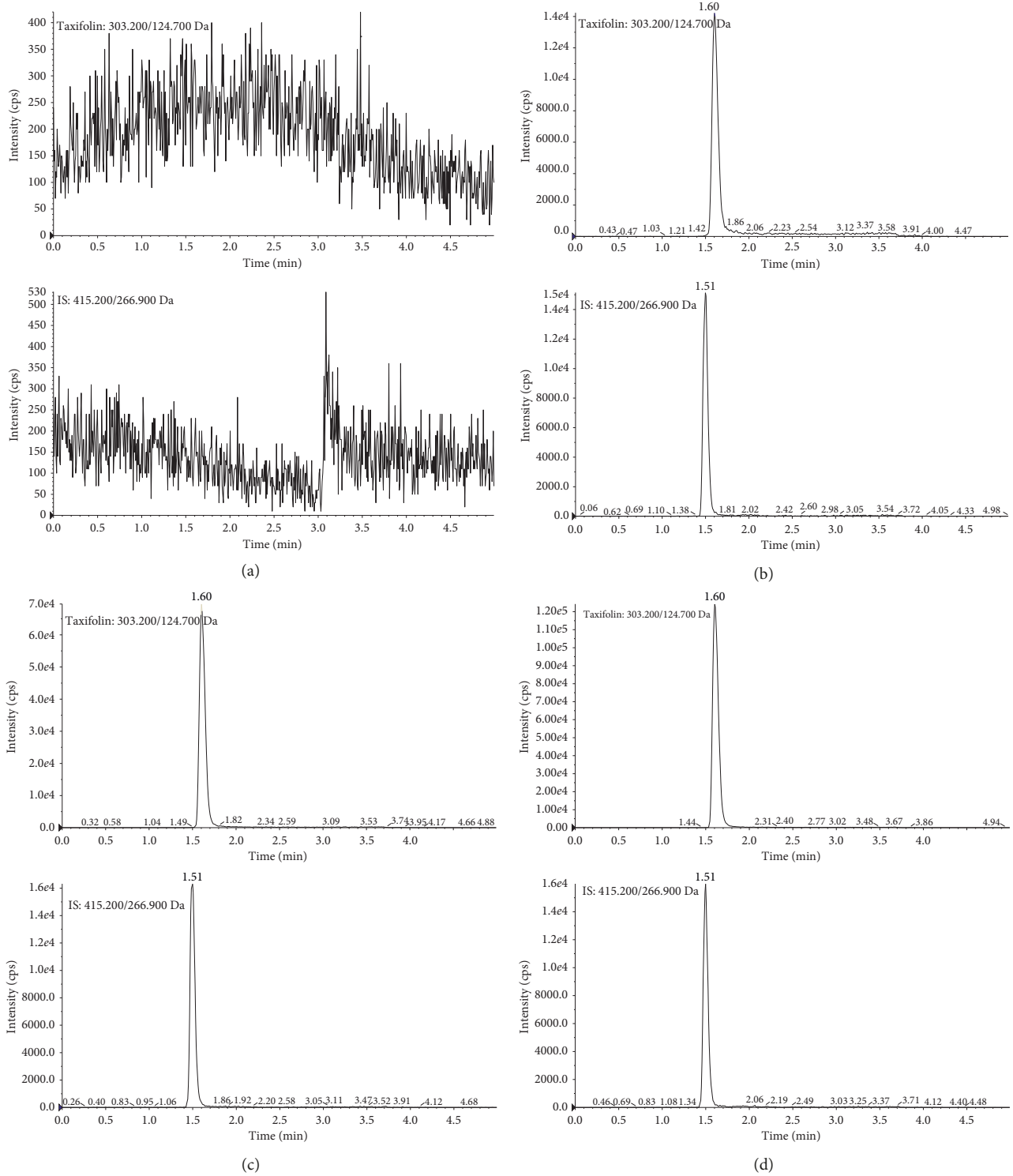


FIGURE 2: Typical chromatograms of (a) blank rat plasma; (b) blank rat plasma spiked with taxifolin (10 ng/mL, LLOQ) and IS; and (c) a normal rat plasma sample collected at 1 h after oral administration of 1.23 g/kg extract of FPO; (d) a model rat plasma sample collected at 10 min after oral administration of 1.23 g/kg extract of FPO.

TABLE 2: Liver function and serum liver fibrosis indexes after PS treatment for 12 weeks ($n = 3$).

Characterize	ALT (IU/L)	AST (IU/L)	HA (pg/mL)	LN (ng/mL)	IV-C (ng/mL)	PCIII (ng/mL)
Normal	37.10 ± 9.45	97.96 ± 11.33	247.09 ± 15.72	5.74 ± 1.58	34.76 ± 1.11	11.71 ± 0.84
Model	72.95 ± 21.10	173 ± 59.29	291.18 ± 40.44	13.56 ± 1.85	41.53 ± 1.53	17.45 ± 3.47
<i>p</i> value	<0.05	<0.05	<0.01	<0.01	<0.01	<0.01

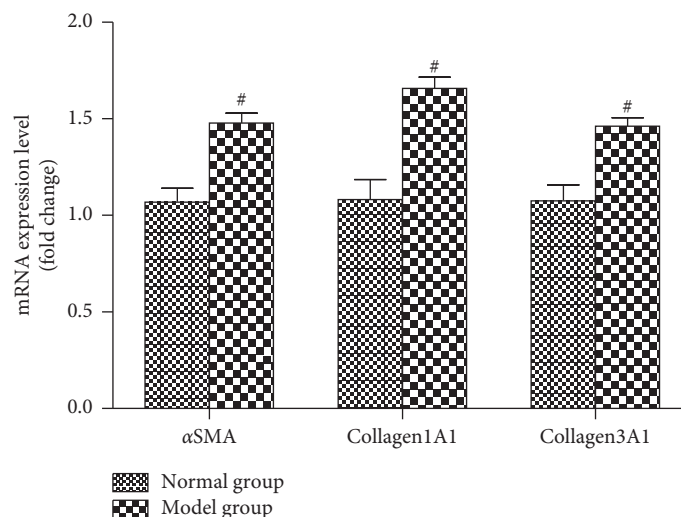


FIGURE 3: The fold change of mRNA expression level of 3 fibrosis-related genes including α SMA, Collagen1A1, and Collagen3A1 in liver tissues detected by qRT-PCR after PS treatment for 12 weeks. Data are expressed as mean \pm SD ($n=3$). [#] $p < 0.05$.

pathologic grading III [26]. There were no obvious pathological changes observed in the normal groups. These results are shown in Figure 4.

3.3. Method Validation

3.3.1. Specificity. The typical chromatograms of a blank plasma sample, an LLOQ sample, and *in vitro* plasma samples after administration of taxifolin are presented in Figure 2. Clearly, there was no significant endogenous interference at the retention times of taxifolin and IS, which indicates that the assay was selective.

3.3.2. Linearity and LLOQ. The linear ranges of taxifolin in rat plasma ranged from 10 to 5000 ng/mL. The calibration curve for taxifolin had a correlation coefficient (r) of 0.995 or better. The lower limit of quantification (LLOQ) of taxifolin was 10 ng/mL.

3.3.3. Precision and Accuracy. The intraday and interday precisions were defined as relative standard deviation (% RSD) with criteria of less than 15%; the accuracy was assessed by comparing the measured concentration with its nominal value using a criterion of $\pm 15\%$ for all QC samples. The results are summarized in Table 3.

3.3.4. Extraction Recovery and Matrix Effect. The extraction recovery and matrix effect results are summarized in Table 4. A mean percentage matrix effect value of 95.9% for taxifolin was calculated and found to be independent of taxifolin plasma concentration and rat plasma lot. This result is in agreement with international guidelines and indicates low ion suppression.

3.3.5. Stability. The described stability data are summarized in Table 5. The results indicated that taxifolin at the three

concentrations tested had acceptable stability after storage at room temperature for 24 h, three cycles of freeze-thaw, and -80°C for 1 month with % RSD values of less than 15%.

3.4. Pharmacokinetic Parameter Comparison. This sensitivity and specificity method was applied to the pharmacokinetic study. The plasma concentration-time profiles of taxifolin in rats are shown in Figure 5. The main pharmacokinetic parameters for normal and fibrotic rats are summarized in Table 6. The peak plasma concentration (C_{\max}), area under the plasma concentration-time curve from time zero to C_{\max} (AUC_{0-t}), area under the plasma concentration-time curve from time zero to infinity ($\text{AUC}_{0-\infty}$), and mean residence time (MRT) in fibrotic rats were markedly increased. The C_{\max} was 1940 ± 502.2 ng/mL and 2648 ± 208.5 ng/mL, respectively; the AUC_{0-t} was 4949.7 ± 764.89 h ng/mL and 6679.9 ± 734.26 h ng/mL ($p < 0.05$); the $\text{AUC}_{0-\infty}$ was 5049.4 ± 760.7 and 7095.2 ± 962.3 h ng/mL ($p < 0.05$); and the MRT of taxifolin was 2.46 ± 0.412 h and 3.17 ± 0.039 h ($p < 0.05$).

4. Discussion

Polygonum plants contain a variety of bioactive substances, mainly flavonoids, which have biological activities including scavenging of free radicals, antioxidant activity, and anti-tumor activity [27]. Taxifolin and quercetin are two important flavonoids in FPO [28, 29]. Studies have shown that the concentration of taxifolin is about ten times higher than that of quercetin in fructus polygoni orientalis [29, 30]. In our preliminary experiment, after oral administration of FPO extract, the taxifolin in plasma was much higher than that of quercetin (data not shown). Therefore, in this study, we mainly detected and compared the absorption of taxifolin into the blood and the pharmacokinetic changes in normal and liver fibrosis rats after oral administration of FPO extract. A UPLC-MS/MS method for quantification of taxifolin in rat plasma was developed and validated. The method

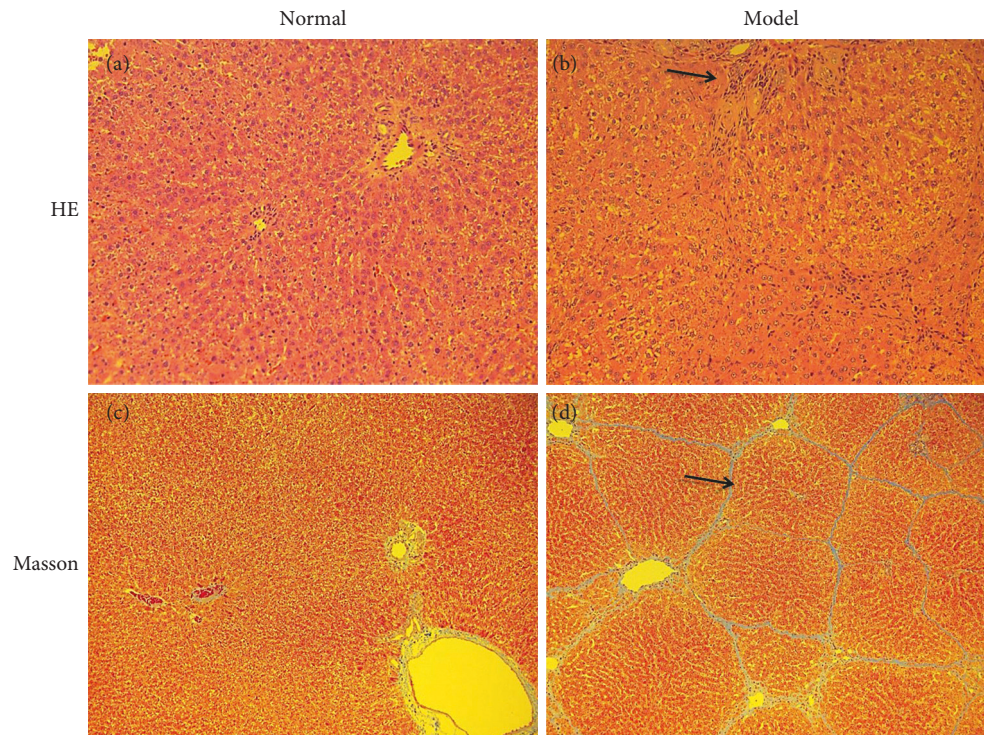


FIGURE 4: Photomicrographs of liver sections stained by (H&E) and Masson's trichrome staining (magnification 200x). Representative histological images of H&E stained rat liver tissue in the (a) normal group (normal), (b) PS-induced fibrotic group (model), respectively. Arrows indicate inflammatory cells infiltration. Representative histological images of Masson's trichrome stained rat liver tissue in the liver tissue in the (c) normal group (normal), (d) PS-induced fibrotic group (model), respectively. Arrows indicate the collagen fibers between the portal region and pseudolobules.

TABLE 3: Intra- and interday precision and accuracy of taxifolin in rat plasma (intraday: 6 replicates at each concentration; interday: 18 replicates at each concentration).

Concentration (ng/mL)	Intraday ($n=6$)			Interday ($n=6 \times 3$)		
	Measured concentration (ng/mL)	Precision (RSD, %)	Accuracy (RE, %)	Measured concentration (ng/mL)	Precision (RSD, %)	Accuracy (RE, %)
10	9.3 ± 1.1	11.8	7.5	8.8 ± 1.1	12.5	12.0
50	47.9 ± 3.3	6.9	4.1	48.6 ± 3.5	7.1	2.8
1000	981.8 ± 42.9	4.4	1.8	999.2 ± 42.9	4.3	0.1
4000	3886.4 ± 106.2	2.7	2.8	3821.4 ± 117.4	3.1	4.5

TABLE 4: The mean recoveries and matrix of taxifolin and the internal standard in rat plasma ($n=6$).

Spiked concentration (ng/mL)	Recovery (%)	RSD (%)	Matrix effect (%)	RSD (%)
50	93.5	5.1	97.8	6.6
1000	94.6	4.5	95.9	5.6
4000	96.2	2.4	97.9	3

TABLE 5: Stability of taxifolin in rat plasma under a variety of storage conditions ($n=3$).

Spiked concentration (ng/mL)	Room temperature for 24 h		Three freeze-thaw cycles		-20°C for 1 month	
	Measured concentration (ng/mL)	RE (%)	Measured concentration (ng/mL)	RE (%)	Measured concentration (ng/mL)	RE (%)
50	49.7 ± 4.9	-0.7	50.9 ± 1.1	1.7	51.1 ± 2.2	2.1
1000	1021.7 ± 41.8	2.2	963.4 ± 45.7	-3.7	949.3 ± 34.4	-5.1
4000	3846.3 ± 99.5	-3.8	3878.3 ± 89.9	-3.0	3766.7 ± 120.2	-5.8

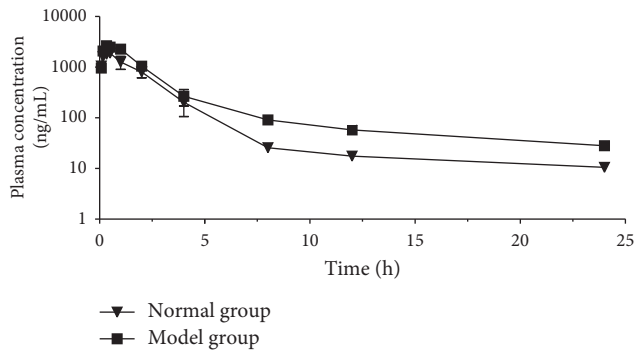


FIGURE 5: Mean plasma concentration-time profiles of taxifolin determined by the UPLC-MS/MS method after oral administration of FPO extract to rats. Each point represents the mean \pm SD ($n = 3$).

TABLE 6: Main pharmacokinetic parameters of taxifolin in rats determined after oral administration of 1.23 g/kg FPO extract ($n = 3$, mean \pm SD).

Parameters	Unit	Normal group	Model group	P value
$t_{1/2}$	h	14.66 \pm 5.11	9.77 \pm 4.19	0.269
T_{max}	h	0.44 \pm 0.096	0.33 \pm 0	0.116
C_{max}	ng/mL	1940 \pm 502.2	2648 \pm 208.5	0.044 [#]
$AUC_{(0 \rightarrow t)}$	h-ng/mL	4949.7 \pm 764.89	6679.9 \pm 734.26	0.048 [#]
$AUC_{(0 \rightarrow \infty)}$	h-ng/mL	5049.4 \pm 760.7	7095.2 \pm 962.3	0.045 [#]
F	%	5.778 \pm 4.01	5.64 \pm 2.77	0.963
V_z	mL/kg	73912 \pm 45956.3	48327 \pm 15259.3	0.428
Cl	mL/h	3382.4 \pm 740.8	3538 \pm 533.7	0.856
Ke	1/h	0.0524 \pm 0.0219	0.0799 \pm 0.0321	0.287
AUC_{INF_pred}	h-ng/mL	4513 \pm 1580.7	7073.7 \pm 947.6	0.074
MRT _{last}	h	2.46 \pm 0.412	3.17 \pm 0.039	0.04 [#]

[#] $p < 0.05$.

showed adequate quantitative ranges, selectivity, linearity, accuracy, and precision. The recoveries and the matrix effects were suitable for quantitation. In brief, this method is suitable for the PK measurement.

The results showed that taxifolin can be absorbed into the blood after oral administration of FPO extract in both normal and hepatic fibrotic model rats. A previous study showed that after the rabbits were given different doses of taxifolin, it could be absorbed into blood, and T_{max} was consistent with our results. However, there were some differences in other pharmacokinetics, including $t_{1/2}$, C_{max} , $AUC_{(0 \rightarrow t)}$, and $AUC_{(0 \rightarrow \infty)}$, which were all higher in our results [31]. The causes for these differences may be as follows: first, the animal models are inconsistent between the two studies, which may influence the absorption process of taxifolin. Second, the ingredients were not the same, and it is not clear whether there are some interactions between the compounds in FPO. Therefore, in clinical practices, the FPO is usually used in treatment of liver diseases instead of taxifolin alone. Taxifolin is one of the most effective flavonoids in silymarin and is a

powerful hepatoprotective agent [32]. We inferred that taxifolin should be the most effective component in the FPO extract. The presence of liver injury has a significant impact on pharmacodynamics and pharmacokinetics [33, 34]. In this study, porcine serum-induced hepatic fibrotic model rats were built successfully after 12 weeks treatment. The PS-induced rat model is characterized by minor hepatocyte damage but intense immune response, and the mechanisms of fibrogenesis are similar to those of hepatic diseases in humans, especially viral hepatitis, which is one of the main causes of liver fibrosis in China [22, 35–38]. Our results indicate that liver fibrosis significantly altered the PK of taxifolin *in vivo* after oral administration of the FPO extract. The pharmacokinetic parameters of single-dose carvedilol changed in hepatic fibrosis when a CCl₄ hepatic fibrosis model was used to study the antifibrosis and pharmacokinetic effects of carvedilol, which are manifested as delayed clearance and drug accumulation. This is thought to result from the decrease of CYP2D6 expression in the hepatic blood flow and liver [39, 40]. The C_{max} and AUC alteration in this study might have been affected by changes in drug absorption, and the delayed MRT might have been the result of drug clearance [41, 42].

5. Conclusion

In conclusion, we found that taxifolin can be absorbed into the blood and that hepatic fibrosis affects the pharmacokinetics of taxifolin after oral administration of the FPO extract. Therefore, personalized dosage adjustment should be considered in clinical practice, especially in patients with serious liver disease conditions.

Data Availability

The data used to support the findings of this study are included within the article.

Conflicts of Interest

The authors declare that there are no conflicts of interests regarding the publication of this paper.

Acknowledgments

The research work was financially supported by the National Natural Science Foundation of China (grant nos. 81773860 and 71473360).

References

- [1] S. L. Friedman, "Mechanisms of hepatic fibrogenesis," *Gastroenterology*, vol. 134, no. 6, pp. 1655–1669, 2008.
- [2] Y. A. Lee, M. C. Wallace, and S. L. Friedman, "Pathobiology of liver fibrosis: a translational success story," *GUT*, vol. 64, no. 5, pp. 830–841, 2015.
- [3] M. M. Aydin and K. C. Akcali, "Liver fibrosis," *The Turkish Journal of Gastroenterology*, vol. 29, no. 1, pp. 14–21, 2018.
- [4] M. Parola and M. Pinzani, "Liver fibrosis: pathophysiology, pathogenetic targets and clinical issues," *Molecular Aspects of Medicine*, vol. 65, pp. 37–55, 2019.

- [5] J. P. Iredale and L. Campana, "Regression of liver fibrosis," *Seminars in Liver Disease*, vol. 37, no. 1, pp. 1–10, 2017.
- [6] F. Tacke and R. Weiskirchen, "An update on the recent advances in antifibrotic therapy," *Expert Review of Gastroenterology & Hepatology*, vol. 12, no. 11, pp. 1143–1152, 2018.
- [7] S. Chu, H. Zhang, and L. Ding, "Efficiency of *Sophora flavescens*-*fructus ligustri lucidi* drug pairs in the treatment of liver fibrosis based on the response surface method," *Evidence-Based Complementary and Alternative Medicine*, vol. 2019, Article ID 8609490, 9 pages, 2019.
- [8] G. P. Caviglia, C. Rosso, S. Fagoonee, G. M. Saracco, and R. Pellicano, "Liver fibrosis: the 2017 state of art," *Panminerva Medica*, vol. 59, no. 4, pp. 320–331, 2017.
- [9] D. Schuppan, M. Ashfaq-Khan, A. T. Yang, and Y. O. Kim, "Liver fibrosis: direct antifibrotic agents and targeted therapies," *Matrix Biology*, vol. 68–69, pp. 435–451, 2018.
- [10] K. Nishikawa, Y. Osawa, and K. Kimura, "Wnt/ β -Catenin signaling as a potential target for the treatment of liver cirrhosis using antifibrotic drugs," *International Journal of Molecular Sciences*, vol. 19, no. 10, p. 3103, 2018.
- [11] N. Ikenaga, Z.-W. Peng, K. A. Vaid et al., "Selective targeting of lysyl oxidase-like 2 (LOXL2) suppresses hepatic fibrosis progression and accelerates its reversal," *GUT*, vol. 66, no. 9, pp. 1697–1708, 2017.
- [12] Y.-J. Chiu, S.-C. Chou, C.-S. Chiu et al., "Hepatoprotective effect of the ethanol extract of *Polygonum orientale* on carbon tetrachloride-induced acute liver injury in mice," *Journal of Food and Drug Analysis*, vol. 26, no. 1, pp. 369–379, 2018.
- [13] Y. N. Tan, M. M. Tong, Y. Y. Zhang, Y. Y. Xu, and Y. J. Zhai, "Determination of taxifolin in *Polygonum orientale* of different storage period," *Zhongguo Zhong Yao Za Zhi*, vol. 38, no. 17, pp. 2779–2781, 2013.
- [14] H. Shin, Y. Park, Y. H. Jeon, X.-T. Yan, and K. Y. Lee, "Identification of *Polygonum orientale* constituents using high-performance liquid chromatography high-resolution tandem mass spectrometry," *Bioscience, Biotechnology, and Biochemistry*, vol. 82, no. 1, pp. 15–21, 2018.
- [15] J. Chen, X. Sun, T. Xia, Q. Mao, and L. Zhong, "Pretreatment with dihydroquercetin, a dietary flavonoid, protected against concanavalin A-induced immunological hepatic injury in mice and TNF- α /ActD-induced apoptosis in HepG2 cells," *Food & Function*, vol. 9, no. 4, pp. 2341–2352, 2018.
- [16] M. Zhao, J. Chen, P. Zhu et al., "Dihydroquercetin (DHQ) ameliorated concanavalin A-induced mouse experimental fulminant hepatitis and enhanced HO-1 expression through MAPK/Nrf2 antioxidant pathway in RAW cells," *International Immunopharmacology*, vol. 28, no. 2, pp. 938–944, 2015.
- [17] I. Ahiskali, C. L. Pinar, M. Kiki, M. Cankaya, C. S. Kunak, and D. Altuner, "Effect of taxifolin on methanol induced oxidative and inflammatory optic nerve damage in rats," *Cutaneous and Ocular Toxicology*, vol. 38, no. 4, pp. 384–389, 2019.
- [18] R. A. Weersink, K. Taxis, J. P. H. Drenth, E. Houben, H. J. Metselaar, and S. D. Borgsteede, "Prevalence of drug prescriptions and potential safety in patients with cirrhosis: a retrospective real-world study," *Drug Safety*, vol. 42, no. 4, pp. 539–546, 2019.
- [19] R. A. Weersink, M. Bouma, D. M. Burger et al., "Evidence-based recommendations to improve the safe use of drugs in patients with liver cirrhosis," *Drug Safety*, vol. 41, no. 6, pp. 603–613, 2018.
- [20] R. A. Weersink, M. Bouma, D. M. Burger et al., "Evaluating the safety and dosing of drugs in patients with liver cirrhosis by literature review and expert opinion," *BMJ Open*, vol. 6, no. 10, Article ID e12991, 2016.
- [21] R. A. Weersink, M. Bouma, D. M. Burger et al., "Safe use of proton pump inhibitors in patients with cirrhosis," *British Journal of Clinical Pharmacology*, vol. 84, no. 8, pp. 1806–1820, 2018.
- [22] Y. Peng, L. Li, X. Zhang et al., "Fluorofenidone affects hepatic stellate cell activation in hepatic fibrosis by targeting the TGF- β 1/Smad and MAPK signaling pathways," *Experimental and Therapeutic Medicine*, vol. 18, no. 1, pp. 41–48, 2019.
- [23] L. Chen, Q. Weng, and J. Ma, "A New UPLC-MS/MS method validated for quantification of jervine in rat plasma and the study of its pharmacokinetics in rats," *Journal of Analytical Methods in Chemistry*, vol. 2019, no. 6, Article ID 5163625, 2019.
- [24] S. H. Jeong, J. H. Jang, and Y. B. Lee, "A novel and sensitive UPLC-MS/MS method to determine mequitazine in rat plasma and urine: validation and its application to pharmacokinetic studies," *Biomedical Chromatography*, vol. 33, no. 10, Article ID e4627, 2019.
- [25] Y. Tao, S. Huang, J. Yan, and B. Cai, "Establishment of a rapid and sensitive UPLC-MS/MS method for pharmacokinetic determination of nine alkaloids of crude and processed *Corydalis turtschaninowii* Besser aqueous extracts in rat plasma," *Journal of Chromatography B*, vol. 1124, pp. 218–225, 2019.
- [26] P. J. Scheuer, "Classification of chronic viral hepatitis: a need for reassessment," *Journal of Hepatology*, vol. 13, no. 3, pp. 372–374, 1991.
- [27] J. Cai, S. Xie, J. Feng, F. Wang, and Q. Xu, "Protective effect of *Polygonum orientale* L. extracts against *Clavibacter michiganense* subsp. *sepedonicum*, the causal agent of bacterial ring rot of potato," *PLoS One*, vol. 8, no. 7, Article ID e68480, 2013.
- [28] Y. Zhai, M. Zhao, H. Zhang, Z. Chu, and T. Kang, "Study on HPLC-FPS of raw and processed *fructus polygoni orientalis*," *Zhongguo Zhong Yao Za Zhi*, vol. 35, no. 6, pp. 711–713, 2010.
- [29] Q. Liu, S. Shi, L. Liu, H. Yang, W. Su, and X. Chen, "Separation and purification of bovine serum albumin binders from *Fructus polygoni orientalis* using off-line two-dimensional complexation high-speed counter-current chromatography target-guided by ligand fishing," *Journal of Chromatography A*, vol. 1304, pp. 183–193, 2013.
- [30] X. Y. Zhou, B. H. Su, Y. Y. Zhang, and Y. J. Zhai, "Effects of different processing on active components in *fructus polygoni orientalis* by HPLC analysis," *Zhong Yao Cai*, vol. 35, no. 4, pp. 540–542, 2012.
- [31] O. N. Pozharitskaya, M. V. Karlina, A. N. Shikov, V. M. Kosman, M. N. Makarova, and V. G. Makarov, "Determination and pharmacokinetic study of taxifolin in rabbit plasma by high-performance liquid chromatography," *Phytomedicine*, vol. 16, no. 2–3, pp. 244–251, 2009.
- [32] K. Anthony and M. Saleh, "Free radical scavenging and antioxidant activities of silymarin components," *Antioxidants*, vol. 2, no. 4, pp. 398–407, 2013.
- [33] R. L. Fitzpatrick, J. M. Quimby, K. K. Benson et al., "In vivo and in vitro assessment of mirtazapine pharmacokinetics in cats with liver disease," *Journal of Veterinary Internal Medicine*, vol. 32, no. 6, pp. 1951–1957, 2018.
- [34] J. Marcinak, M. Vakilynejad, A. Kogame, and Y. Tagawa, "Evaluation of the pharmacokinetics and safety of a single oral dose of fasilglifam in subjects with mild or moderate hepatic impairment," *Drugs in R&D*, vol. 18, no. 2, pp. 109–118, 2018.
- [35] Q. Huang, X. Zhang, F. Bai et al., "Methyl helicerte ameliorates liver fibrosis by regulating miR-21-mediated ERK and TGF- β 1/Smads pathways," *International immunopharmacology*, vol. 66, pp. 41–51, 2019.
- [36] A. Shiga, K. Shiota, T. Ikeda, and Y. Nomura, "Morphological and immunohistochemical studies on porcine serum-

- induced rat liver fibrosis,” *Journal of Veterinary Medical Science*, vol. 59, no. 3, pp. 159–167, 1997.
- [37] Y. Baba, K. Uetsuka, H. Nakayama, and K. Doi, “Rat strain differences in the early stage of porcine-serum-induced hepatic fibrosis,” *Experimental and Toxicologic Pathology*, vol. 55, no. 5, pp. 325–330, 2004.
- [38] S. Ge, X. Wang, J. Xie, X. Yi, and F. Liu, “Deep sequencing analysis of microRNA expression in porcine serum-induced hepatic fibrosis rats,” *Annals of Hepatology*, vol. 13, no. 4, pp. 439–449, 2014.
- [39] E. El-Demerdash, S. A. Abdel-Sattar, W. M. El-Bakly, and E. A. Mohamed, “Antifibrotic effects of carvedilol and impact of liver fibrosis on carvedilol pharmacokinetics in a rat model,” *European Journal of Drug Metabolism and Pharmacokinetics*, vol. 42, no. 5, pp. 767–779, 2017.
- [40] M. B. Abrudan, D. M. Muntean, A. M. Gheldiu, M. A. Neag, and L. Vlase, “The pharmacokinetic interaction study between carvedilol and bupropion in rats,” *Pharmacology*, vol. 99, no. 3-4, pp. 139–143, 2017.
- [41] J. Zhang, X.-Y. Wen, and R.-P. Gao, “Hepatitis B virus-related liver cirrhosis complicated with dermatomyositis: a case report,” *World Journal of Clinical Cases*, vol. 7, no. 10, pp. 1206–1212, 2019.
- [42] E. Cheema, A. Al-Aryan, and A. Al-Hamid, “Medicine use and medicine-related problems in patients with liver cirrhosis: a systematic review of quantitative and qualitative studies,” *European Journal of Clinical Pharmacology*, vol. 75, no. 8, pp. 1047–1058, 2019.



Hindawi

Submit your manuscripts at
www.hindawi.com

